ACS OMEGA

http://pubs.acs.org/journal/acsodf

Article

Facile Supramolecular Engineering of Porphyrin cis Tautomers: The Case of β-Octabromo-*meso*-tetraarylporphyrins

Kolle E. Thomas, Carla Slebodnick,* and Abhik Ghosh*

Cite This: *ACS Omega* 2020, 5, 8893–8901

Read Online

ACCESS | Metrics & More | Article Recommendations | Supporting Information

ABSTRACT: A porphyrin cis tautomer, where the two central NH protons are on adjacent pyrrole rings, has long been invoked as an intermediate in porphyrin tautomerism. Only recently, however, has such a species been isolated and structurally characterized. Thus, single-crystal X-ray structure determinations of two highly saddled free-base porphyrins, β-heptakis(trifluoromethyl)-*meso*-tetrakis(*p*-fluorophenyl)porphyrin, $H_2[(CF_3)_7TFPP]$, and β-octaiodo-5,10,15,20-tetrakis(4′-trifluoromethylphenyl)porphyrin, $H_2[I_8TCF_3PP]$, unambiguously revealed cis tautomeric structures, each stabilized as a termolecular complex with a pair of ROH (R = CH_3 or H) molecules that form hydrogen-bonded N−H···O−H···N straps connecting the central NH groups with the antipodal unprotonated nitrogens. The unusual substitution patterns of these two porphyrins, however, have left open the question how readily such supramolecular assemblies might be engineered, which prompted us to examine the much more synthetically accessible β-octabromo-*meso*-tetraphenylporphyrins. Herein, single-crystal X-ray structures were obtained for two such compounds, 2,3,7,8,12,13,17,18-octabromo-5,10,15,20-tetrakis(4′-trifluoromethylphenyl)-porphyrin, $H_2[Br_8TCF_3PP]$, and 2,3,7,8,12,13,17,18-octabromo-5,10,15,20-tetrakis(4′-fluorophenyl)porphyrin, $H_2[Br_8TFPP]$, and although the central hydrogens could not all be located unambiguously, the electron density could be convincingly modeled as porphyrin cis tautomers, existing in each case as a bis-methanol adduct. In addition, a perusal of the Cambridge Structural Database suggests that there may well be additional examples of porphyrin cis tautomers that have not been recognized as such. We are therefore increasingly confident that porphyrin cis tautomers are readily accessible via supramolecular engineering, involving the simple stratagem of crystallizing a strongly saddled porphyrin from a solvent system containing an amphiprotic species such as water or an alcohol.

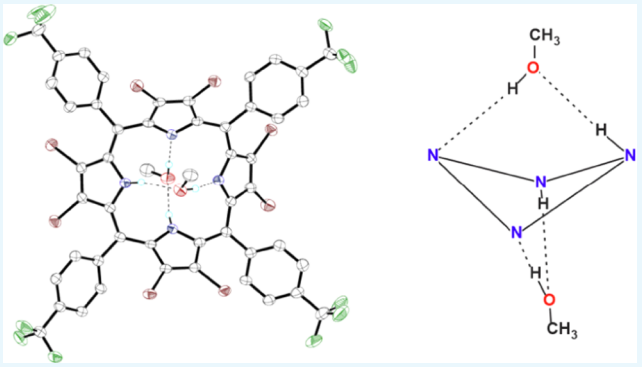

INTRODUCTION

Kinetic[1−3] and quantum chemical[4,5] studies have long implicated the cis tautomer as an intermediate in porphyrin tautomerism, but the species have eluded direct observation until very recently. The recent breakthrough happened in the course of single-crystal X-ray structure determinations of two highly saddled free-base porphyrins, β-heptakis-(trifluoromethyl)-*meso*-tetrakis(*p*-fluorophenyl)porphyrin, $H_2[(CF_3)_7TFPP]$ (CSD: TATQEN),[6] and β-octaiodo-5,10,15,20-tetrakis(4′-trifluoromethylphenyl)porphyrin, $H_2[I_8TCF_3PP]$ (JIKJAR),[7] each crystallized in the presence of a hydroxylic solvent. In each case, the structures revealed a termolecular complex consisting of the porphyrin cis tautomer and an ROH molecule strapped across each macrocycle face, which stabilized the NHs in a hydrogen-bond network. The central hydrogens were explicitly located in both structures, unambiguously confirming the successful isolation of the cis porphyrin tautomer. Given the rather unusual substitution patterns of these two porphyrins, which are rather inaccessible from a synthetic point of view, we were interested in finding cis tautomers among more readily available free-base porphyrins. Accordingly, we turned our attention to free-base β-octabromo-*meso*-tetraphenylporphyrins,[8,9] which can be synthesized quite straightforwardly, a strategy that proved rewarding. We obtained single-crystal X-ray structures of two such porphyrins as bis-methanol adducts, namely, 2,3,7,8,12,13,17,18-octabromo-5,10,15,20-tetrakis(4′-trifluoromethylphenyl)porphyrin, $H_2[Br_8TCF_3PP]\cdot 2CH_3OH$,[10] and 2,3,7,8,12,13,17,18-octabromo-5,10,15,20-tetrakis(4′-fluorophenyl)porphyrin, $H_2[Br_8TFPP]\cdot 2CH_3OH$. Although the central hydrogens in the two structures could not all be unambiguously located, they nonetheless could be convincingly modeled as porphyrin cis tautomers (Table 1). Furthermore, a perusal of the Cambridge Structural Database (CSD)[11] suggests that there may well be

Received: February 5, 2020
Accepted: March 24, 2020
Published: April 2, 2020

https://dx.doi.org/10.1021/acsomega.0c00517
ACS Omega 2020, 5, 8893−8901

Table 1. Crystal and Structure Refinement Data

	$H_2[Br_8TCF_3PP]\cdot 2CH_3OH$	$H_2[Br_8TFPP]\cdot 2CH_3OH$
chemical formula	$C_{48}H_{18}Br_8F_{12}N_4\cdot 2CH_3OH$	$C_{44}H_{18}Br_8F_4N_4\cdot 2CH_3OH$
formula weight	1582.03	1381.99
T (K)	99.99(11)	100.00(10)
λ (Å)	1.54184 (Cu Kα)	0.71073 (Mo Kα)
crystal system	monoclinic	tetragonal
space group	$P12_1/c1$	$I4_1/a$
a (Å)	36.7959(4)	20.8825(5)
b (Å)	10.19901(8)	20.8825(5)
c (Å)	30.7172(3)	10.1100(3)
β (deg)	112.8497(11)°	
volume (Å^3)	10623.00(19)	4408.8(2)
Z, Z'	8, 2	4, 1/4
ρ (calc) (g·cm^{-3})	1.978	2.082
μ (mm^{-1})	7.997	7.339
$F(000)$	6064	2648
crystal size (mm^3)	0.011 × 0.098 × 0.124	0.122 × 0.200 × 0.443
θ range (deg)	3.823−77.524	3.903−30.495
index ranges	$-46 \le h \le 46$, $-12 \le k \le 11$, $-3 \le l \le 38$	$-29 \le h \le 28$, $-29 \le k \le 29$, $-14 \le l \le 11$
measured reflections	177057	21857
unique reflections	22336 [R(int) = 0.0737]	3361 [R(int) = 0.0532]
completeness	100.0% (to θ = 67.684°)	99.7% (to θ = 25.242°)
absorption correction	Gaussian	Gaussian
max. and min. transmission	1.000 and 0.413	0.446 and 0.190
data/restraints/parameters	22 336/153/1505	3361/0/152
S (GooF) on F^2 (all data)	1.127	1.071
R1 [$I > 2\sigma(I)$], w$R2$ (all data)	0.0476, 0.1209	0.0703, 0.1878
R indices (all data)	0.0528, 0.1241	0.0990, 0.2051
Max/min residence density (e·Å^{-3})	1.062/−0.634	3.147/−1.946

additional examples of porphyrin cis tautomers that have not been recognized as such (e.g., HOCMOB).[12] We are thus led to conclude that porphyrin cis tautomers are far from unique or even rare but may be stabilized and isolated in a predictable manner, potentially opening the door to applications in such fields as organocatalysis and molecular sensing.[13]

RESULTS AND DISCUSSION

Figures 1 and 2 depict the anisotropic displacement ellipsoid diagrams for the two free-base porphyrin structures analyzed in this study, namely, $H_2[Br_8TCF_3PP]\cdot 2CH_3OH$ and $H_2[Br_8TFPP]\cdot 2CH_3OH$. These two structures represent the third and fourth reported examples of porphyrin cis tautomers. The two new structures are entirely analogous to the two earlier structures and exhibit the two key features identified as necessary for a stable cis tautomer: (1) a strongly saddled macrocycle conformation and (2) a hydroxylic or amphiprotic solvent that enables transannular N−H···X−H···N hydrogen bonding on both faces of the porphyrin.

Saddling distortions can be quantified by measuring the dihedral angle between the $C_\beta-C_\alpha$ and $C_{\alpha'}-C_{\beta'}$ vectors of the adjacent pyrrole ring. For a planar porphyrin, these dihedrals will be zero. For saddled porphyrins, the dihedral will have alternating positive and negative values going around the ring, with the magnitude of the angles providing a measure of the saddling; the larger the magnitude, the greater the distortion. For $H_2[Br_8TCF_3PP]\cdot 2CH_3OH$, the magnitude of the dihedral angles ranges from 97.3(10) to 104.1(9)° and 91.6(11) to 100.9(10)° for the two crystallographically independent molecules. For $H_2[Br_8TFPP]\cdot 2CH_3OH$, because of crystallographic symmetry constraints, the saddling dihedrals are equal in magnitude, with a value of 91.4°. Table 2 summarizes the saddling dihedrals for the two new structures, the two previously reported porphyrin cis tautomers,[6,7] and from one additional structure[12] from the literature with strong saddling and a bridging amphiprotic molecule.

For the two previously reported porphyrin cis tautomers,[6,7] the central hydrogen atoms were reliably located and found to participate in a transannular N−H···X−H···N bonding pattern on both sides of the porphyrin macrocycle. For $H_2[(CF_3)_7TFPP]$, the bridging solvent was H_2O, and for $H_2[I_8TCF_3PP]$, the solvent was CH_3OH on one face and disordered CH_3OH/H_2O on the opposite face. For both the present structures, the solvent is CH_3OH. Thus, all four cis tautomers have an N−H···O−H···N transannular hydrogen-bonding pattern.

For $H_2[Br_8TCF_3PP]\cdot 2CH_3OH$, seven of eight hydrogen atoms involved in the N−H···O−H···N hydrogen-bond networks (two networks from each of the two crystallographically independent molecules) were located experimentally. Because the difference electron peaks used to locate the hydrogen atoms were weak, the corresponding atom positions were not assigned at the same confidence level as for the two earlier structures. (See the Supporting Information for a detailed procedure for locating and refining the hydrogen-atom positions.) All of the hydrogen-atom locations were, however, consistent with cis porphyrin tautomers.

For $H_2[Br_8TFPP]\cdot 2CH_3OH$, the crystallographically imposed symmetry required the N−H hydrogens to be disordered across all four porphyrin nitrogens, each at 50% occupancy. Similarly, the methanol was disordered across a twofold symmetry position requiring an O−H hydrogen disorder, with each hydrogen atom at 50% occupancy. This disorder made it impossible to formally prove the existence of the cis tautomer by locating the hydrogen atoms. A careful analysis of the possible hydrogen-bonding motifs for the cis and trans tautomers, however, demonstrated that only the cis tautomer gives a chemically reasonable hydrogen-bonding pattern (vide infra). Table 3 summarizes the hydrogen-bonding distances and angles for the two structures reported here. Figure 3 provides an expanded view of the hydrogen-bonding networks for the two unique molecules of $H_2[Br_8TCF_3PP]\cdot 2CH_3OH$, while Figure 4 provides an alternative schematic representation of the transannular hydrogen bonding in both new structures.

Our inability to locate the methanol OH hydrogens led to an ambiguity as to whether the correct structure is the doubly solvated, neutral porphyrin, $H_2[Por]\cdot 2CH_3OH$, or the porphyrin diacid with methoxide counterions, $[H_4Por][OCH_3]_2$. The latter species is readily rejected on chemical grounds, since a weak base such as a free base porphyrin (assuming a pK_b similar to pyridine, i.e., ∼5) is not expected to deprotonate a weak acid such as methanol (pK_a = 15.5).

The reader may find it useful to explicitly consider the possible hydrogen-bonding networks for porphyrin trans tautomers. Figure 5a depicts two equally contributing structures that average to give the disorder model shown in Figure 4b. In this model, a hydrogen-bond network is generated by protonating

https://dx.doi.org/10.1021/acsomega.0c00517
ACS Omega 2020, 5, 8893−8901

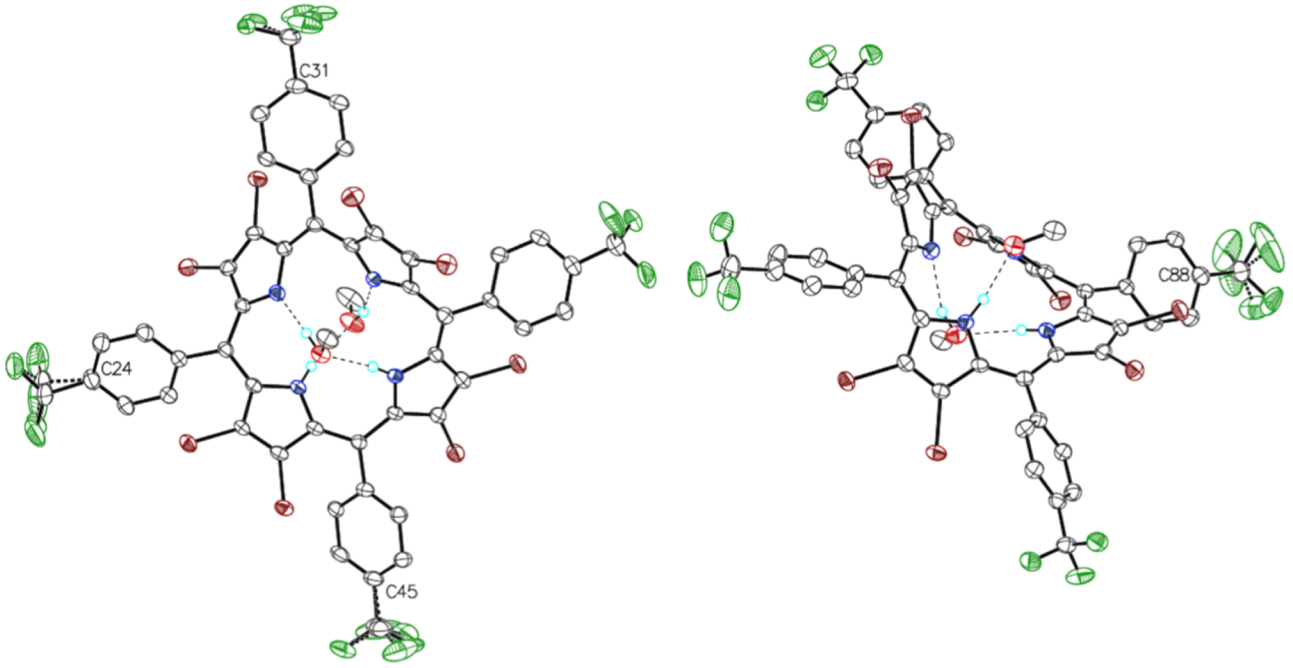

Figure 1. Anisotropic displacement ellipsoid drawing (50% probability) depicting the two crystallographically unique molecules in the asymmetric unit of $H_2[Br_8TCF_3PP]\cdot 2CH_3OH$. The C−H hydrogens are omitted for clarity. The CF_3 groups connected to C24, C31, C45, and C88 were modeled with 2-position disorder with relative occupancies that refined to 0.708(15)/0.292(15), 0.62(4)/0.38(4), 0.75(2)/0.25(2), and 0.63(4)/0.37(4), respectively.

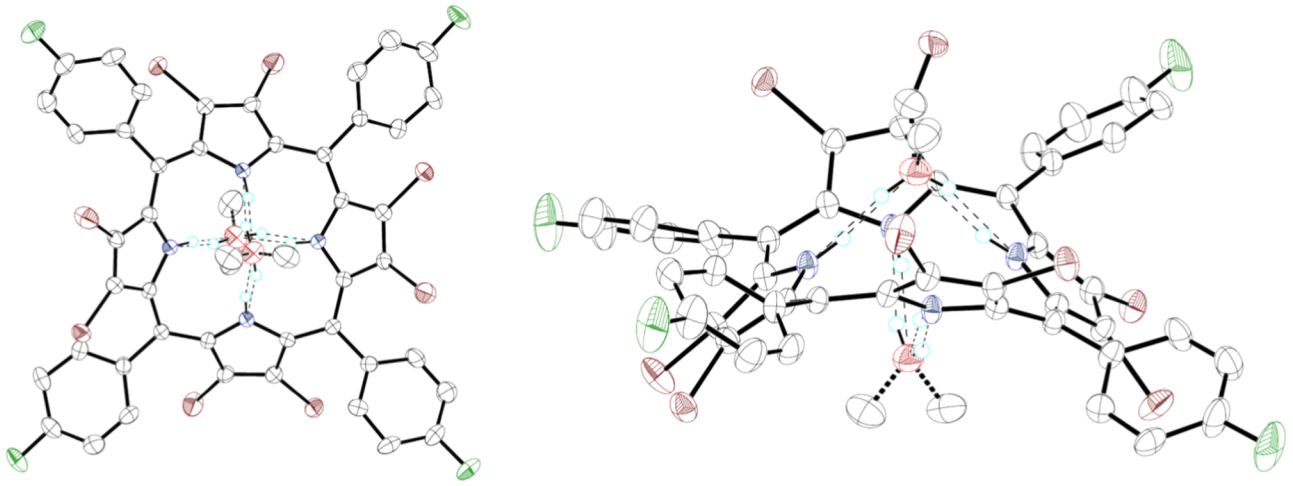

Figure 2. Anisotropic displacement ellipsoid drawing (50% probability) for $H_2[Br_8TFPP]$. The C−H hydrogens are omitted for clarity. The methanol C- and H-atoms and the pyrrole H-atoms are disordered and constrained to 50% occupancy by symmetry. Left: top view. Right: side view.

Table 2. Summary of $C_\beta-C_\alpha-C_{\alpha'}-C_{\beta'}$ Dihedral Angles in Known and Plausible *cis* Porphyrin Structures

	meso-substituent	β-substituent	solvent(s) or other amphiprotic species	angles (deg)
$H_2[Br_8TCF_3PP]$, molecule 1	4-F−C_6H_4	Br	CH_3OH	−104.1, 97.3, −98.8, 101.8
$H_2[Br_8TCF_3PP]$, molecule 2	4-F−C_6H_4	Br	CH_3OH	100.9, −98.2, 91.6, −95.7
$H_2[Br_8TFPP]$	4-CF_3−C_6H_4	Br	CH_3OH	91.3, −91.3, 91.3, −91.3
TATQEN	4-F−C_6H_4	7(CF_3), 1H	H_2O	117.7, −118.5, 116.5, −114.1
JIKJAR	4-CF_3−C_6H_4	I	CH_3OH, H_2O	−107.4, 106.5, −97.7, 100.5
HOCMOB	Ph	Ph	EtOH	106.6, −108.0, 98.3, −93.13

one methanol to give $CH_3OH_2^+$ and deprotonating another methanol to give CH_3O^-, an unlikely scenario that we deemed chemically unreasonable. Figure 5b shows two of the four equally contributing conformations that also average to give the disorder model in Figure 4b. In this model, the methanol on the "protonated" face of the saddled *trans* tautomer acts as an acceptor for both N−H protons, with the OH hydrogen directed away from the porphyrin and not participating in any hydrogen bonding. The methanol on the "unprotonated" face can then form a hydrogen bond to only one nitrogen, leaving an N···O

https://dx.doi.org/10.1021/acsomega.0c00517
ACS Omega 2020, 5, 8893−8901

Table 3. Hydrogen-Bond Geometries (Å and deg)

D−H···A	*d*(D−H)	*d*(H···A)	*d*(D···A)	∠(DHA)
		$H_2[Br_8TCF_3PP]\cdot 2CH_3OH$		
N(1)−H(1)···O(1)	0.88(2)	1.95(3)	2.812(5)	166(6)
N(4)−H(4)···O(2)	0.87(2)	1.98(2)	2.844(5)	173(5)
N(5)−H(5)···O(4)	0.87(2)	1.95(3)	2.797(5)	165(6)
N(8)−H(8)···O(3)	0.87(2)	2.07(3)	2.923(5)	166(6)
O(1)−H(1S)···N(3)	0.83(2)	2.09(3)	2.894(5)	164(6)
O(2)−H(2S)···N(2)	0.84(2)	2.11(4)	2.908(5)	159(8)
O(3)−H(3S)···N(6)	0.859(19)	2.022(19)	2.837(5)	158(6)
O(4)−H(4S)···N(7)	0.84(2)	2.05(2)	2.884(5)	174(9)
		$H_2[Br_8TFPP]\cdot 2CH_3OH$		
N(1)−H(1)···O(1)	0.88	2.00	2.862(7)	168.2
O(1)−H(1A)···N(1)#1[a]	0.84	2.05	2.862(7)	161.9

[a]Symmetry transformations used to generate equivalent atoms: #1 $-x + 1, -y + 1/2, z$.

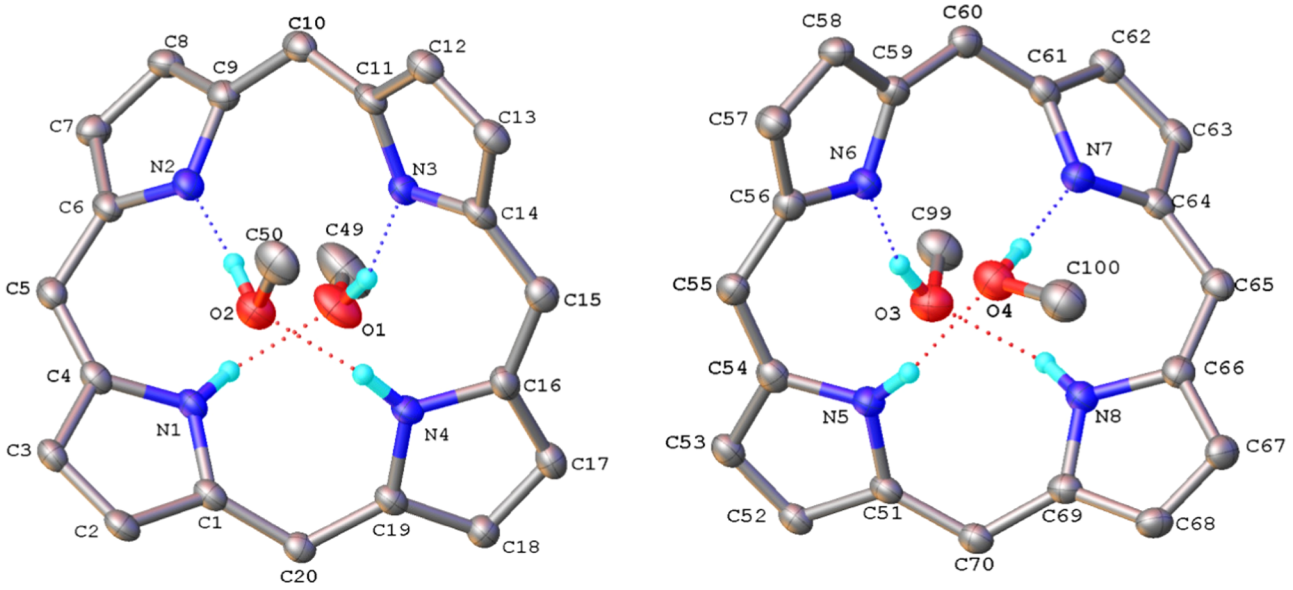

Figure 3. Expanded view of the hydrogen-bonding networks in the two molecules of the asymmetric unit of $H_2[Br_8TCF_3PP]\cdot 2CH_3OH$.

within hydrogen-bonding distance [2.862(7) Å] but not actually participating in hydrogen bonding. A symmetric hydrogen bond with the hydrogen atom equidistant from the two nitrogen atoms was considered but is not reasonable, as it would require a C−O−H angle of ∼143°, which deviates substantially from the ideal tetrahedral angle of 109.5°. In addition, the O−H···N angle was estimated at ∼120°, well below the expected range of ∼150−180° for medium-to-strong hydrogen bonds.

Figure 6 depicts four equally contributing conformations of a porphyrin cis tautomer that average to give the disorder model depicted in Figure 4b. Each conformation gives a reasonable hydrogen-bonding motif with neutral methanol to form the transannular N−H···X−H···N hydrogen-bonding network proposed in our earlier work.

A longstanding observation worth recalling in this connection is that the C_α−N−C_α angles serve as an indirect but quite reliable probe of the *N*-protonation sites in free-base porphyrins, with unprotonated pyrrole groups exhibiting C_α−N−C_α angles in the 106−108° range and protonated pyrrole groups exhibiting C_α−N−C_α angles in the 110−112° range.[14−20] For the two crystallographically unique molecules of $H_2[Br_8TCF_3PP]\cdot 2CH_3OH$, the angles for the putative protonated pyrrole rings are 111.0(3), 111.0(3), 111.3(4), and 110.5(4)° and those for putative unprotonated pyrrole rings are 107.4(4), 107.4(3), 107.8(4), and 107.2(4)°, in excellent agreement with structural precedent. For $H_2[Br_8TFPP]\cdot 2CH_3OH$, the C_α−N−C_α angle is 109.0(5)°, a reasonable value considering that the disorder model entails an averaging of two protonated and two unprotonated pyrrole rings.

With four porphyrin cis tautomers documented by us (including the two here), a question that begs to be answered is "how many more might there be in the literature?". This question proved more difficult to answer than expected for multiple reasons. First, the N−H hydrogen-atom positions are often difficult or impossible to locate in X-ray crystal structures. Positional disorder is common. Porphyrins also commonly crystallize with solvents that are disordered, which contributes to the difficulty in assigning hydrogen-atom positions. Second, even when the X-ray diffraction data are good, porphyrin chemists have generally taken for granted that free-base porphyrins are *trans* tautomers and have not concerned themselves with the hydrogen-atom positions in crystal structures. Third, a surprising number of porphyrin structures in the CSD have incorrect occupancies assigned to the N−H hydrogen atoms and the chemical formulas of disordered solvents. In such cases, the structure reported in the paper does

https://dx.doi.org/10.1021/acsomega.0c00517
ACS Omega 2020, 5, 8893−8901

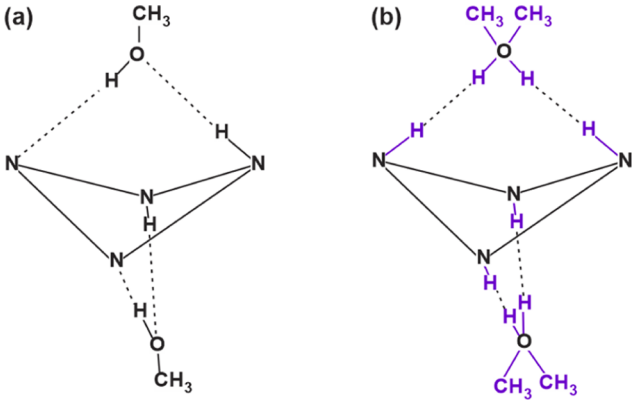

Figure 4. Simplified schematic representation of the two structures obtained in this work. The four nitrogen atoms connected by solid lines represent the saddle-shaped porphyrin. The two CH_3OH solent molecules are poised directly above and below the porphyrin, with each methanol oxygen within hydrogen-bonding distance of a pair of trans nitrogen atoms of the porphyrin. (a) Depiction of the hydrogen-bonding network in $H_2[Br_8TCF_3PP]\cdot 2CH_3OH$ modeled as an ordered cis tautomer. (b) Disorder model in $H_2[Br_8TFPP]\cdot 2CH_3OH$. Atoms in purple are at 50% occupancy. Careful analysis of the disorder is necessary to deduce chemically reasonable hydrogen-bonding networks.

not match the structure and/or chemical formula in the CIF, making substructure searches inefficient.

After extensive searching in the CSD, only one additional convincing example of a cis tautomer was identified (HOCMOB[12]). Many similar examples were identified, however, in the form of monoprotonated[21,22] and diprotonated[22−25] porphyrins with carboxylate counterions. These protonated porphyrins exhibit essentially the same transannular bonding motif as the cis tautomers. Thus, whereas the cis tautomers have N−H···X−H···N linkages, the analogous linkages in the protonated porphyrins are better represented as N−H···X···H−N, i.e., the key difference is in the relative distance of the hydrogen atoms from the porphyrin nitrogen atoms vs. the amphiprotic bridging ligand. If the hydrogen atoms are closer to the bridging solvent, the system is best viewed as an $H_2[Por]\cdot 2HX$ cis tautomer. If one or both are closer to the pyrrole nitrogens, the system is better described as $H_3[Por]^+\cdot X^-\cdot HX$ or $H_4[Por]^{2+}\cdot 2X^-$, with the relative pK_as determining the product formed.

An interesting twist to the above story is provided by the structure of free-base 2,3,12,13-tetrachloro-5,7,8,10,15,17,18,20-octaphenylporphyrin·$2CH_3OH$ (SUNXIJ).[26] The structure satisfies our stated criteria for cis tautomer formation, namely, a strongly saddled porphyrin macrocycle and the presence of an amphiprotic solvent. Yet, a different hydrogen-bond pattern forms, one that stabilizes the *trans* tautomer (Figure 7). Compared with the cis-tautomer structures, the methanol molecules in SUNXIJ also form hydrogen bonds with each other (O1−H···O2 in Figure 7). As a result, the oxygen atom O1 is only available to the porphyrin as a hydrogen-bond acceptor and does so for both NH units (N2 and N4) of the *trans* tautomer. The second methanol is displaced off-center relative to the porphyrin core and forms a hydrogen bond with only one of the unprotonated nitrogens (O2−H···N1). Atom N3 of the porphyrin is not involved in any hydrogen bonding, with the closest nonbonded distance being to the methyl hydrogen of C70 (HC70···N3 = 2.525 Å). Thus, although a saddling distortion and an amphiprotic solvent are required, they do not guarantee the formation of a cis tautomer.

The reason SUNXIJ does not form a cis tautomer is most probably because of the electronic effects of antipodal *β*-tetrachloro substitution. Several additional examples are known where antipodal *β*-tetrahalogenation freezes NH tautomerism and unambiguously localizes the central NH hydrogens on the unhalogenated pyrrole rings.[27] These observations beg the question of whether certain substituents by themselves might be able to stabilize the cis tautomer. Density functional theory calculations in one of our laboratories suggest that the answer is "yes, but exceedingly rarely."[28]

CONCLUSIONS

Although the locations of the central hydrogens of the two structures reported here could not be unambiguously assigned, the electron density could be satisfactorily modeled in terms of porphyrin cis tautomers. The structures are stabilized by transannular hydrogen bonding with methanol exactly as previously observed in our two earlier reports. In all cases, the

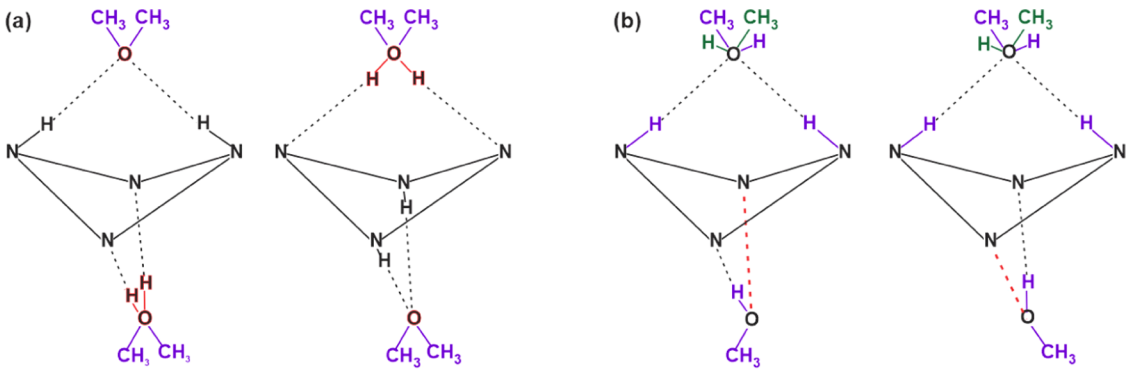

Figure 5. Two trans tautomer models. (a) Two equally contributing *trans*-conformation models that average to give the structure in Figure 4b. To obtain reasonable hydrogen-bonding motifs in this model, each contributing structure must have a protonated ($CH_3OH_2^+$) and a deprotonated (CH_3O^-) "methanol." These chemically unreasonable components are highlighted in red. (b) Two of the four equally contributing *trans* tautomer models with the methanol hydrogen on the protonated side of the saddle-shaped porphyrin oriented away from the *trans* N−H atoms to give a satisfactory hydrogen-bonding motif on that face. The opposite face, however, has a close N···O distance, 2.862(7) Å (red dotted line), with no hydrogen atom involved in a hydrogen bond. The green and purple atoms represent two different conformations of the disordered methanol. The two other equally contributing conformations are not shown but shown are the equivalent structures with the other pair of nitrogen atoms protonated.

https://dx.doi.org/10.1021/acsomega.0c00517
ACS Omega 2020, 5, 8893−8901

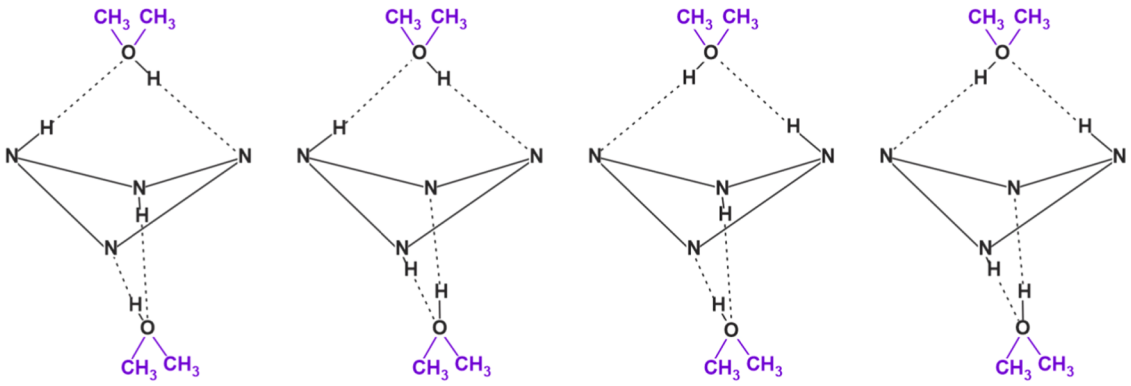

Figure 6. Four equally contributing conformations for $H_2[Br_8TFPP]\cdot 2CH_3OH$. Disordered groups, each at 50% occupancy, are shown in purple. The cis tautomer is the only form that gives a chemically reasonable hydrogen-bonding model with neutral methanol. Upon averaging, the four structures depicted above give the disorder model shown in Figure 4b.

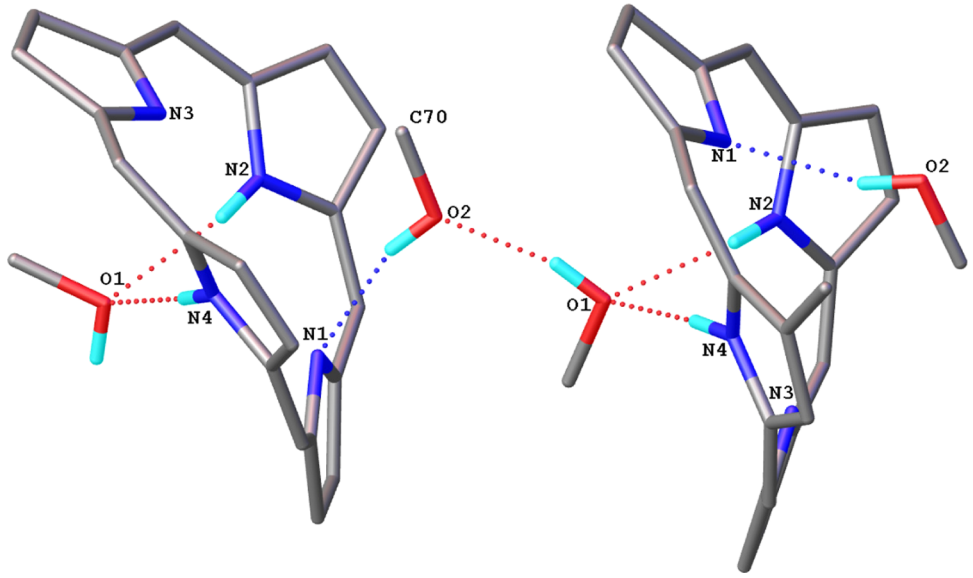

Figure 7. Crystal structure of the SUNXIJ porphyrin core and methanol solvate depicting the hydrogen-bonding network.

key requirements appear to be a strongly saddled porphyrin macrocycle and a pair of hydroxylic or amphiprotic solvent molecules providing the critical transannular N−H···X−H···N straps that stabilize the cis tautomer. With four examples now reported by us and at least an additional one in the literature, porphyrin cis tautomers may be regarded as relatively readily accessible from appropriate substrates crystallized from suitable amphiprotic solvents. Besides broadening our appreciation of hydrogen bonding, tautomerism, and crystal/supramolecular engineering, can porphyrin tautomers prove useful in a practical sense? Can supramolecular assemblies of the type disclosed here provide a platform for the sensing of alcohols and other amphiprotic hydrogen-bond donors or for that matter for organocatalysis? Also, as chiral assemblies with a C_2 axis along a pair of opposite meso carbons, might these constructs exhibit interesting chiroptical properties? These remain fascinating questions for the future.

EXPERIMENTAL SECTION

Materials and Instrumentation. All reagents and solvents were used as purchased, except pyrrole, which was predried and distilled from CaH_2 under vacuum. Silica (150 Å pore size, 35−70 μm particle size, Davisil) and both neutral and basic alumina (activity I) were used for column (flash) chromatography.

Ultraviolet−visible spectra were recorded on an HP 8453 spectrophotometer in CH_2Cl_2 at room temperature. NMR spectra were recorded on a Mercury Plus Varian spectrometer (400 MHz for ^{1}H and 376 MHz for ^{19}F) at 298 K. ^{19}F shifts (δ) in ppm were referenced to 2,2,2-trifluoroethanol-d_3 ($\delta = -77.8$ ppm). Mass spectra were recorded on a Waters Micromass matrix-assisted laser desorption/ionization (MALDI) Micro MX mass spectrometer with α-cyano-4-hydroxycinnamic acid as the matrix.

Syntheses. *Meso*-tetrakis(4-fluorophenyl)porphyrin, $H_2[TFPP]$, and *meso*-tetrakis(4-trifluoromethylphenyl)-porphyrin, $H_2[TCF_3PP]$, were synthesized via modified[29,30] Adler−Longo[31] procedures. The corresponding Cu complexes were prepared by refluxing the free bases overnight with $Cu(OAc)_2\cdot H_2O$ (10 equiv) in DMF and purified via flash chromatography as described for copper tetraphenylporphyrin.[32] The copper octabromoporphyrins $Cu[Br_8TXPP]$ (X = F, CF_3) were prepared following a literature protocol.[33] To obtain $Cu[Br_8TFPP]$, Cu[TFPP] was brominated in $CHCl_3$ with 24 equiv Br_2 over 4 h. For $Cu[Br_8TCF_3PP]$, complete β-bromination was accomplished overnight with 80 equiv Br_2.

https://dx.doi.org/10.1021/acsomega.0c00517
ACS Omega 2020, 5, 8893−8901

The free-base octabromoporphyrins $H_2[Br_8TXPP]$ (X = F, CF_3) were then prepared via demetallation of the corresponding Cu complexes with HBr in 1:1 v/v chloroform/trifluoroacetic acid (TFA),[34] as described in detail below for the known compound $H_2[Br_8TCF_3PP]$.

2,3,7,8,12,13,17,18-Octabromo-5,10,15,20-tetrakis(4-trifluoromethylphenyl)porphyrin, $H_2[Br_8TCF_3PP]$. To a solution of $Cu[Br_8TCF_3P]$ (100 mg) in $CHCl_3$ (10 mL), TFA (99+%, 10 mL) was added, followed by 6 drops of HBr (33% in acetic acid). After stirring for 1 h, the mixture was washed with distilled water (40 mL x 3) and extracted with $CHCl_3$. The $CHCl_3$ phase was washed twice with saturated aqueous $NaHCO_3$ (40 mL each time), dried with anhydrous Na_2SO_4, and filtered, and the filtrate was rotary-evaporated to dryness. The residue obtained was crystallized from 1:2 $CHCl_3$/*n*-hexane to give analytically pure bluish-green needles of the target compound. Yield: 90 mg (94%). All spectroscopic data matched those reported earlier.[10] Rectangular crystals suitable for X-ray structure determination were obtained from evaporation of a 1:1 *n*-hexane/CH_2Cl_2 solution of the porphyrin with traces of methanol within 2 weeks.

2,3,7,8,12,13,17,18-Octabromo-5,10,15,20-tetrakis(4-fluorophenyl)porphyrin, $H_2[Br_8TFPP]$. The green residue obtained after work-up was crystallized from 1:1 $CHCl_3$/CH_3OH yielding an analytically pure, green solid (83 mg, 86%). UV−vis λ_{max} (nm; $\varepsilon \times 10^{-4}$, M^{-1} cm^{-1}): 365 (2.41), 465 (15.77), 571 (0.98), 622 (0.75), 729 (0.28). ^1H NMR δ (tetrahydrofuran (THF)-d_8, δ 3.58, 1.73 ppm): 8.19 (dd, 8H, 5,10,15,20-*o* or -*m*, J = 8.6 and 5.48 Hz, Ph); 7.53 (t, 8H, J = 8.8 Hz, 5,10,15,20-*m* or -*o*, Ph). ^{19}F NMR δ (THF-d_8): −112.45 to −112.55 (m, 4F). MS (MALDI-TOF, major isotopomer): $[M + H]^+$ = 1318.38 (expt), 1318.49 (calcd). Elemental analysis found (calcd): C 41.50 (40.10), H 1.92 (1.38), N 3.79 (4.25). Diffusion from methanol into a chloroform solution of the compound yielded X-ray-quality rectangular needles in about 2 weeks.

X-ray Structure Determinations. Data sets were collected on a Rigaku Oxford Diffraction Synergy-S diffractometer equipped with a HyPix6000HE detector and operating with Cu Kα radiation ($H_2Br_8TCF_3PP{\cdot}2CH_3OH$) or a Gemini E Ultra diffractometer operating with Mo Kα radiation ($H_2Br_8TFPP{\cdot}2CH_3OH$). An Oxford Cryosystems Cryostream 800 Plus was used to cool the samples to 100 K. The data collection routine, unit cell refinement, and data processing were carried out with the program CrysAlisPro.[35] The structures were solved using SHELXT[36] and refined using SHELXL[37] via Olex2.[38] The crystal data and structure refinement data are summarized in Table 1. Olex 2 was used for generating molecular graphics.

In the X-ray analysis of $H_2[Br_8TCF_3PP]{\cdot}2CH_3OH$, a brown plate (0.01 × 0.10 × 0.12 mm^3) was chosen for analysis. The crystal had a minor twin component (~5%). With such a small component, attempts to process the data as a non-merohedral twin led to poorer refinements so the crystal was treated as a single unit. The Laue symmetry and systematic absences were consistent with the monoclinic space group $P2_1/c$. The asymmetric unit consisted of two porphyrin molecules and four CH_3OH solvent molecules (as shown in Figure 1). Four of the eight unique CF_3 groups were disordered; each was modeled with 2-position disorder with relative occupancies refining to the ratios presented in Figure 1. The SHELX RIGU command was used to maintain reasonable anisotropic displacement ellipsoids for each CF_3 group. In addition, when there was substantial atom overlap in the disordered group, EADP was used to constrain the anisotropic displacement ellipsoids to be equal. A riding model was used for the C−H hydrogen atoms. All four of the N−H hydrogen atoms from porphyrin cores and three of the four O−H hydrogen atoms from the methanol molecules were located experimentally from the difference electron density map. The hydrogen atom bonded to O3 could not be located and was placed in an optimized position for an alcohol −OH. An in-depth discussion of the hydrogen-atom position assignments and refinement is included in the SI. The final refinement model involved anisotropic displacement parameters for nonhydrogen atoms.

For $H_2[Br_8TFPP]{\cdot}2CH_3OH$, a brown rod (0.12 × 0.20 × 0.44 mm^3) was chosen for analysis. The Laue symmetry and systematic absences were consistent with the tetragonal space group $I4_1/a$. The porphyrin was found to have crystallographically imposed $\bar{4}$ symmetry, giving $Z = 4$ and $Z' = 0.25$. The final refinement model involved anisotropic displacement parameters for nonhydrogen atoms. The methanol was modeled with 2-position disorder and relative occupancies were constrained to 50% by symmetry. A riding model was used for the C−H hydrogen atoms. Because of the $\bar{4}$ symmetry of the porphyrin (Wyckoff position *4a*, origin choice 2), and to maintain charge neutrality on the porphyrin ring, the N−H atoms were by necessity disordered across the four nitrogen atoms in the structure model, each at 50% occupancy. Similarly, the methanol was disordered across a twofold symmetry position (Wyckoff position 8*e*) requiring a O−H hydrogen disorder, with each hydrogen atom at 50% occupancy. Attempts to locate the disordered hydrogen atoms from the difference electron density map were unsuccessful, even when looking at the ∞−1.5 Å data, where the hydrogen atom scattering is a stronger contributor to the structure factors. In the final refinement model, the one crystallographically unique N−H hydrogen was constrained with AFIX 43 (aromatic nitrogen) and the one unique methanol O−H hydrogen was constrained with AFIX 147 (idealized O−H group with torsion angle defined to place the hydrogen atom at the position of maximum electron density).

■ ASSOCIATED CONTENT

Supporting Information

The Supporting Information is available free of charge at https://pubs.acs.org/doi/10.1021/acsomega.0c00517.

NMR, mass, and UV−vis spectra, crystallographic data (PDF)

cs2041_final2 (CIF)

cs2495_final2 (CIF)

Accession Codes

The crystal structures reported in this paper have been deposited at the Cambridge Crystallographic Data Centre and assigned the deposition numbers CCDC 1979194-1979195.

■ AUTHOR INFORMATION

Corresponding Authors

Carla Slebodnick − *Department of Chemistry, Virginia Tech, Blacksburg, Virginia 24601, United States;* orcid.org/0000-0003-4188-7595; Email: slebod@vt.edu

Abhik Ghosh − *Department of Chemistry, UiT—The Arctic University of Norway, 9037 Tromsø, Norway;* orcid.org/0000-0003-1161-6364; Email: abhik.ghosh@uit.no

https://dx.doi.org/10.1021/acsomega.0c00517
ACS Omega 2020, 5, 8893−8901

Author

Kolle E. Thomas − *Department of Chemistry, UiT—The Arctic University of Norway, 9037 Tromsø, Norway*

Complete contact information is available at: https://pubs.acs.org/10.1021/acsomega.0c00517

Notes

The authors declare no competing financial interest.

■ ACKNOWLEDGMENTS

This work was supported by the Research Council of Norway (grant no. 262229) and the U. S. National Science Foundation (grant no. CHE-1726077). We thank Dr. Laura J. M^{c}Cormick-M^{c}Pherson for helpful discussions.

■ REFERENCES

(1) Limbach, H. H.; Lopez, J. M.; Kohen, M. Arrhenius Curves of Hydrogen Transfers: Tunnel Effects, Isotope Effects and Effects of Pre-Equilibria. *Philos. Trans. R. Soc. B* **2006**, *361*, 1399−1415.

(2) Butenhoff, T. J.; Moore, C. B. Hydrogen Atom Tunneling in the Thermal Tautomerism of Porphine Imbedded in a *n*-Hexane Matrix. *J. Am. Chem. Soc.* **1988**, *110*, 8336−8341.

(3) Butenhoff, T.; Chuck, R.; Limbach, H.-H.; Moore, C. B. Vibrational Photochemistry of Porphine Imbedded in a *n*-Hexane-D_{14} Shpol'skii Matrix. *J. Phys. Chem. A* **1990**, *94*, 7847−7851.

(4) Ghosh, A.; Almlöf, J. Structure and Stability of *cis*-Porphyrin. *J. Phys. Chem. A* **1995**, *99*, 1073−1075.

(5) Maity, D. K.; Bell, R. L.; Truong, T. N. Mechanism and quantum mechanical tunneling effects on inner hydrogen atom transfer in free base porphyrin: A direct ab initio dynamics study. *J. Am. Chem. Soc.* **2000**, *122*, 897−906.

(6) Thomas, K. E.; McCormick, L. J.; Vazquez-Lima, H.; Ghosh, A. Stabilization and Structure of the *Cis* Tautomer of a Free-Base Porphyrin. *Angew. Chem., Int. Ed.* **2017**, *56*, 10088−10092.

(7) Thomassen, I. K.; McCormick, L. J.; Ghosh, A. Molecular Structure of a *β*-Octaiodo-*meso*-tetraarylporphyrin. A Rational Route to *Cis* Porphyrin Tautomers? *Cryst. Growth Des.* **2018**, *18*, 4257−4259.

(8) Dolphin, D.; Traylor, T. G.; Xie, L. G. Polyhaloporphyrins: Unusual Ligands for Metals and Metal-Catalyzed Oxidations. *Acc. Chem. Res.* **1997**, *30*, 251−259.

(9) Ghosh, A.; Halvorsen, I.; Nilsen, H. J.; Steene, E.; Wondimagegn, T.; Lie, E.; van Caemelbecke, E.; Guo, N.; Ou, Z.; Kadish, K. M. Electrochemistry of Nickel and Copper *β*-Octahalogeno-*meso*-tetraarylporphyrins. Evidence for Important Role Played by Saddling-Induced Metal(d_{x2-y2})−Porphyrin("a_{2u}") Orbital Interactions. *J. Phys. Chem. B* **2001**, *105*, 8120−8124.

(10) Suzuki, W.; Kotani, H.; Ishizuka, T.; Shiota, Y.; Yoshizawa, K.; Kojima, T. Formation and Isolation of a Four-Electron-Reduced Porphyrin Derivative by Reduction of a Stable 20*π* Isophlorin. *Angew. Chem., Int. Ed.* **2018**, *57*, 1973−1977.

(11) Groom, C. R.; Bruno, I. J.; Lightfoot, M. P.; Ward, S. C. The Cambridge Structural Database. *Acta Crystallogr., Sect. B: Struct. Sci., Cryst. Eng. Mater.* **2016**, *B72*, 171−179.

(12) Senge, M. Fixation of Neutral Molecules in the Binding Cavity of Nonplanar Porphyrins - A Third Dodecaphenylporphyrin Modification with NH-Solvent Hydrogen Bonding. *Z. Naturforsch.* **1999**, *54b*, 821−824.

(13) Kielmann, M.; Senge, M. O. Molecular Engineering of Free-Base Porphyrins as Ligands − The N−H···X Binding Motif in Tetrapyrroles. *Angew. Chem., Int. Ed.* **2019**, *58*, 418−441.

(14) Fleischer, E. B. Structure of Porphyrins and Metalloporphyrins. *Acc. Chem. Res.* **1970**, *3*, 105−112.

(15) Silvers, S. J.; Tulinsky, A. The Crystal and Molecular Structure of Triclinic Tetraphenyl Porphyrin. *J. Am. Chem. Soc.* **1967**, *89*, 3331−3337.

(16) Codding, P. W.; Tulinsky, A. Structure of Tetra-*n*-propylporphine. Average Structure for the Free Base Macrocycle from Three Independent Determinations. *J. Am. Chem. Soc.* **1972**, *94*, 4151−4157.

(17) Lauher, J. W.; Ibers, J. A. Structure of Ocaethylporphyrin. A Comparison with Other Free Base porphyrins. *J. Am. Chem. Soc.* **1973**, *95*, 5148−5152.

(18) Caughey, W. S.; Ibers, J. A. Crystal and Molecular Structure of the Free Base Porphyrin Protoporphyrin IX Dimethyl Ester. *J. Am. Chem. Soc.* **1977**, *99*, 6639−6645.

(19) Devillers, C. H.; Fleurat-Lessard, P.; Lucas, D. "Porphine," the fully unsubstituted porphyrin: A comprehensive overview, In *Handbook of Porphyrin Science*, Kadish, W.; Smith, K. M.; Guilard, R., Eds.; World Scientific: Singapore, 2014; Vol. *37*, pp 75−231.

(20) Almlöf, J.; Fischer, T. H.; Gassman, P. G.; Ghosh, A.; Häser, M. Electron Correlation in Tetrapyrroles: *Ab Initio* Calculations on Porphyrin and the Tautomers of Chlorin. *J. Phys. Chem. A* **1993**, *97*, 10964−10970.

(21) Honda, T.; Kojima, T.; Fukuzumi, S. Crystal structures and properties of a monoprotonated porphyrin. *Chem. Commun.* **2009**, 4994−4996.

(22) Fukuzumi, S.; Honda, T.; Kojima, T. Structures and photo-induced electron transfer of protonated complexes of porphyrins and metallophthalocyanines. *Coord. Chem. Rev.* **2012**, *256*, 2488−2502.

(23) Stone, A.; Fleischer, E. B. The molecular and crystal structure of porphyrin diacids. *J. Am. Chem. Soc.* **1968**, *90*, 2735−2748.

(24) Cheng, B.; Munro, O. Q.; Marques, H. M.; Scheidt, W. R. An Analysis of Porphyrin Molecular FlexibilityUse of Porphyrin Diacids. *J. Am. Chem. Soc.* **1997**, *119*, 10732−10742.

(25) Juillard, S.; Ferrand, Y.; Simonneux, G.; Toupet, L. Molecular structure of simple mono- and diphenyl meso-substituted porphyrin diacids: influence of protonation and substitution on the distorsion. *Tetrahedron* **2005**, *61*, 3489−3495.

(26) Bhyrappa, P.; Arunkumar, C.; Varghese, B. Influence of Mixed Substituents on the Macrocyclic Ring Distortions of Free Base Porphyrins and Their Metal Complexes. *Inorg. Chem.* **2009**, *48*, 3954−3965.

(27) Ochsenbein, P.; Ayougou, K.; Mandon, D.; Fischer, J.; Weiss, R.; Austin, R. N.; Jayaraj, K.; Gold, A.; Terner, J.; Fajer, J. Conformational Effects on the Redox Potentials of Tetraarylporphyrins Halogenated at the *β*−Pyrrole Positions. *Angew. Chem., Int. Ed.* **1994**, *33*, 348−350.

(28) Thomas, K. E.; Conradie, J.; Beavers, C. M.; Ghosh, A. Free-Base Porphyrins with Localized NH Protons. Can Substituents Alone Stabilize the Elusive *Cis* Tautomer? *Org. Biomol. Chem.* DOI: 10.1039/d0ob00452a (in press).

(29) Asadi, M.; Zabardasti, A. Synthesis, characterisation and spectral studies of some molecular adducts of organotin(IV) chlorides with free base *meso*-tetraarylporphyrins. *J. Chem. Res.* **2002**, *12*, 611−613.

(30) Asano, N.; Uemura, S.; Kinugawa, T.; Akasaka, H.; Mizutani, T. Synthesis of Biladienone and Bilatrienone by Coupled Oxidation of Tetraarylporphyrins. *J. Org. Chem.* **2007**, *72*, 5320−5326.

(31) Adler, A. D.; Longo, F. R.; Finarelli, J. D.; Goldmacher, J.; Assour, J.; Korsakoff, L. A simplified synthesis of *meso*-tetraphenylporphine. *J. Org. Chem.* **1967**, *32*, 476.

(32) Adler, A. D.; Longo, F. R.; Varadi, V.; Little, R. G. Metalloporphyrins. *Inorg. Synth.* **1976**, *16*, 213−220.

(33) Bhyrappa, P.; Krishnan, V. Octabromotetraphenylporphyrin and its metal derivatives: Electronic structure and electrochemical properties. *Inorg. Chem.* **1991**, *30*, 239−245.

(34) Nascimento, E. D.; da Silva, G. F.; da Caetano, F. A.; Pernaut, J. M.; Rebouças, J. S.; Idemori, Y. M. Partially and fully *β*-brominated Mnporphyrins in P450 biomimetic systems: Effects of the degree of bromination on electrochemical and catalytic properties. *J. Inorg. Biochem.* **2005**, *99*, 1193−1204.

(35) *Rigaku Oxford Diffraction; CrysAlisPro*, version 1.171.39.46; Rigaku Corporation: Oxford, U.K., 2018.

(36) Sheldrick, G. M. SHELXT − Integrated space-group and crystal structure determination. *Acta Crystallogr.* **2015**, *A71*, 3−8.

(37) Sheldrick, G. M. Crystal Structure Refinement with SHELXL. *Acta Crystallogr.* **2015**, *A71*, 3−8.

(38) Dolomanov, O. V.; Bourhis, L. J.; Gildea, R. J.; Howard, J. A. K.; Puschmann, H. a complete structure solution, refinement and analysis program/OV Dolomanov. *J. Appl. Crystallogr.* **2009**, *42*, 339−341.

NOTE ADDED AFTER ASAP PUBLICATION

This paper was published ASAP on April 2, 2020, with a Supporting Information PDF document containing incorrect pagination and figure numbering. The corrected version was posted on April 6, 2020.

https://dx.doi.org/10.1021/acsomega.0c00517
ACS Omega 2020, 5, 8893−8901